A Numerical Investigation of Stresses, Printing Efficiency, Printability, and Cell Viability in Nozzle Printheads for 3D Extrusion Bioprinting

3D押し出しバイオプリンティングに関する流体剪断応力、印刷効率、印刷適性、細胞生存率に関する数値解析

ZHANG Colin
M2
Okano Lab.

June 2023

Introduction to 3D Extrusion Bioprinting

- In the field of manufacturing tissues and organs, 3D extrusion bioprinting plays a pivotal role.
- This technique involves using bioinks, a unique type of ink containing living cells.
- A key feature of these bioinks is their shear-thinning behavior, where the viscosity decreases under an increased shear rate.
- Despite being the most popular devices for bioprinting, these systems have significant limitations[1]:

Benefit	**Drawback**
Affordable and scalable	Limited printing resolution and speed
Ease of operation	Produce high stresses inside the needle
Deposit high cell densities	Low cell viability (40–80%)

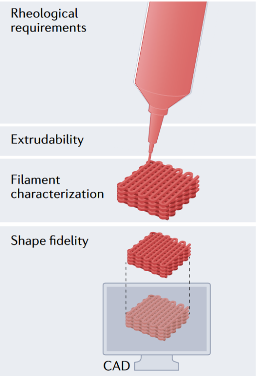

Assessment Criteria of 3D extrusion bioprinting.[1]
*CAD: computer-aided design.

[1] For more details, see Y. S. Zhang et al., *Nature Reviews Methods Primers*, **1**(1), pp. 1–20, 2021

Printing Assessment Criteria

- Controlling stresses in the needle is a key factor to balance:
  - Efficiency/printability
  - Cell viability[2]
- Printing efficiency
  - Extrusion speed
  - Needle moving speed
- Printability
  - Extrudability
  - Shape fidelity

Impediments:

- Difficult to experimentally observe stresses.
- Testing thousands of different bioinks is repetitive.
- The need to optimize cell viability, printing efficiency, and printability.[3]

Objectives:

I. Performing numerical simulation to assess **stresses**, **efficiency/printability**, and **cell viability**.

II. Investigating **needle geometries** and **bioink's rheological properties** to increase cell viability.

[2] Blaeser et al., *Advanced Healthcare Materials*, **5**(3), pp. 326–333, 2016

[3] H. Zhang et al., *Advanced Functional Materials*, **30**(13), p. 1910573, 2020

Part I: Bioink Inside the Needle

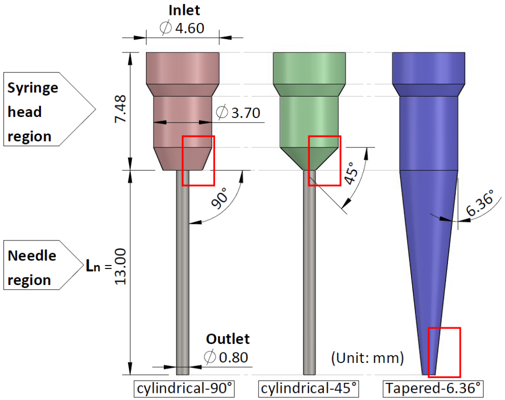

Analytical Model of a Cylindrical Needle

Symbol	Description
τ_{rz}	Shear stress
η	Apparent viscosity
V_z	Velocity along z-axis
r	Variable radius
K	Consistency index
n	Flow index
$\dot{\gamma}$	Shear Rate
R	Needle radius
P	Pressure
ΔP_n	Pressure drop in needle
L_n	Needle length
Q	Volumetric flow rate

Assumptions:

- I Incompressible power-law fluid
- II No-slip smooth wall boundary
- III Negligible gravity influence
- IV Fully developed laminar flow

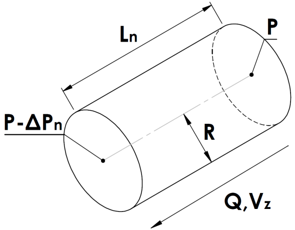

Setup of analytical and simulation validations.

$$\tau_{rz} = \eta\left(\frac{\mathrm{d}V_z}{\mathrm{d}r}\right) = K\dot{\gamma}^n \quad (1)$$

$$\eta = K\dot{\gamma}^{n-1} \quad (2)$$

Open∇FOAM® Simulation Model

- Incompressible continuity equation:

$$\nabla \cdot \boldsymbol{U} = 0$$

- Steady-state Navier–Stokes equations:

$$\boldsymbol{U} \cdot \nabla \boldsymbol{U} - \nabla \cdot \left(\frac{\eta}{\rho} \nabla \boldsymbol{U}\right) = -\frac{\nabla P}{\rho}$$

- Poisson equation for pressure:

$$\frac{\nabla^2 P}{\rho} = \nabla \cdot \left(\frac{\eta}{\rho} \nabla^2 \boldsymbol{U} - \boldsymbol{U} \cdot \nabla \boldsymbol{U}\right)$$

- Power law modified Reynolds number:

$$Re_{PL} = \frac{(2R)^n \bar{U}^{2-n}}{\frac{1}{\rho} K [(3n+1)/(4n)]^n 8^{n-1}}$$

- Shear rate (scalar):

$$\dot{\gamma} = \sqrt{\frac{1}{2} \nabla \boldsymbol{U} : \nabla \boldsymbol{U}}$$

- Power law with a viscosity limiter:

$$\eta = K \dot{\gamma}^{n-1}, \ \eta_{\mathsf{min}} \leq \eta \leq \eta_{\mathsf{max}}$$

Symbol	Description
$\boldsymbol{U}$	Velocity vector
$\bar{U}$	Mean velocity
ρ	Fluid density
$:$	Inner product

Simulation Setup

Parameters

- **Needle Type**: 90° and 45° cylindrical, 6.36° tapered, with volumetric flow rates (Q) of 50 μL/s.
- **Bioink Type**: Alginate-based, chosen due to its wide commercial use, affordability, biocompatibility, and easy gelation process[4].
- **Bioink Properties**: Contains 1 to 4% alginate (w/v) at 25 to 55 °C. Exhibits a consistency coefficient (K) of 29.86 Pa·s^n and a flow behavior index (n) of 0.46.

- Rheological behavior is predominantly driven by the disentanglement and elongation of polymer chains[5].
- Solid line: non-Newtonian shear-thinning behavior.
- Dashed line: yield stress observed outside the needle.

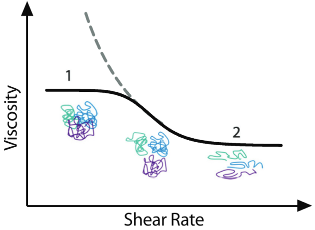

[4] Piras and Smith, *Journal of Materials Chemistry B*,. **8**(36), pp. 8171–8188, 2020

[5] Cooke and Rosenzweig, *APL Bioengineering*, **5**(1), p. 011502, 2021

Stress Dependencies of Temperature

- The 90°, 45°, and tapered datasets represent different stress distributions under the influence of temperature changes.
- Temperature changes significantly affect the stress distribution.
- The 2.5% (w/v) condition shows the effect of temperature change most noticeably.

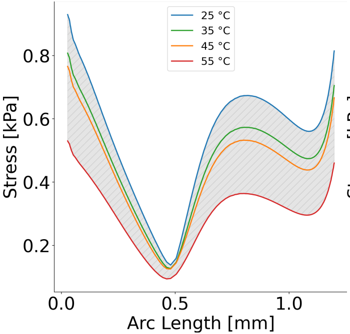

90° cylindrical needle

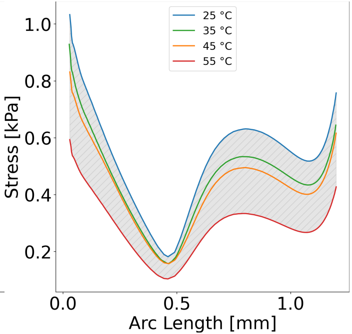

45° cylindrical needle

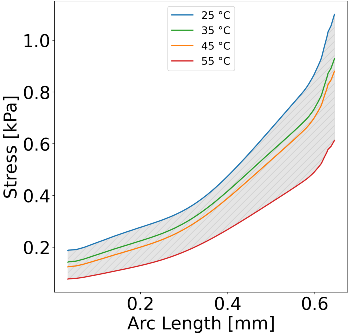

Tapered needle

Part II: Printed Bioink Strand

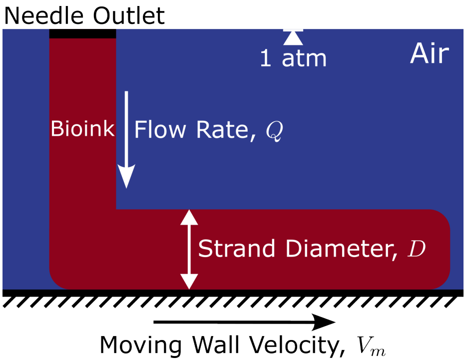

Printing Efficiency and Printability

- **Printing Efficiency**
  - **Extrusion Speed:** the rate at which the bioink is pushed out of the nozzle during printing.
  - **Needle moving speed:** the speed at which the nozzle or needle moves during printing.
- **Printability**
  - **Extrudability:** the ease with which the bioink can be extruded through the nozzle or needle during printing.
  - **Shape Fidelity:** the ability of the printed structure to maintain its shape after deposition.

The Herschel–Bulkley Fluid Model[5,6]

- Herschel–Bulkley fluid: $\tau = \boxed{\sigma_y} + K\dot{\gamma}^n$
- Nonlinear regression of experimental rheological data, where $T_0, T_1, T_2, C_0, C_1, C_2, a, b, d, f, g, h, i, j,$ and m are constants:

$$K = a\exp\left(\frac{T_0}{T} - \frac{C_0}{C}\right) - b\left(\frac{T}{T_0}\frac{C}{C_0}\right) + d\left(\frac{T_0}{T}\right)$$

$$\sigma_y = f\exp\left(\frac{T_1}{T} - \frac{C}{C_1}\right) + g\left(\frac{T_1}{T}\frac{C}{C_1}\right)^{T/T_1} + h\left(\frac{T_1}{T}\right)$$

$$n = i\exp\left(-\frac{T_2}{T} - \frac{C_2}{C}\right) - j\left(\frac{T_2}{T}\frac{C_2}{C}\right) + m\left(\frac{T}{T_2}\right)$$

$$\boxed{25\ ^\circ\mathrm{C} \le T \le 55\ ^\circ\mathrm{C}; 1\%\ (\mathrm{w/v}) \le C \le 4\%\ (\mathrm{w/v})}$$

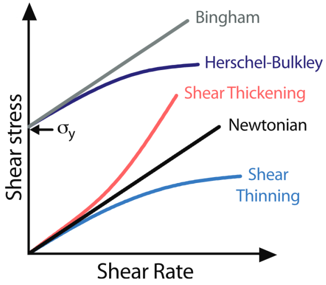

Symbol	Description
σ_y	Yield stress
T	Temperature
C	Mass concentration

[5]Sarker and Chen, *Journal of Manufacturing Science and Engineering*, **139**(8), p. 081002, 2017

Experimental Validation on 2.5% (w/v) Alginate-based Bioink

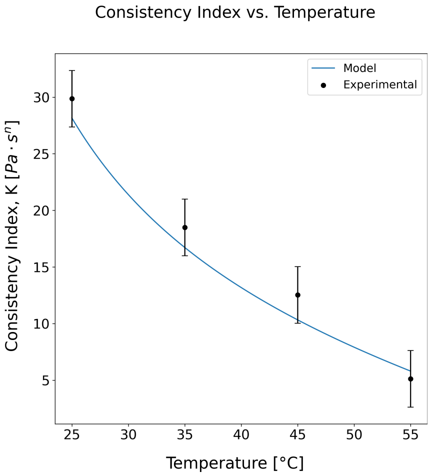

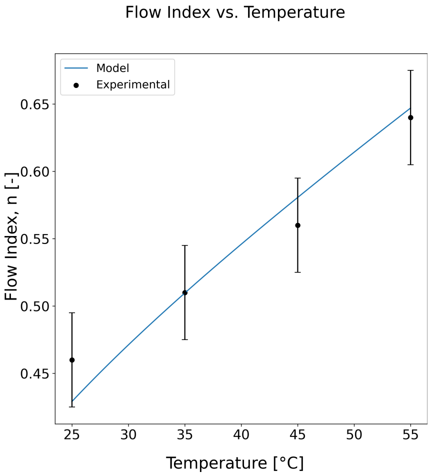

Governing Equations for Printed Bioink Strand

- $\nabla \cdot \boldsymbol{V} = 0$ (Incompressible continuity equation)
- $\rho \frac{\partial \mathbf{V}}{\partial t} + \rho \boldsymbol{V} \cdot \nabla \boldsymbol{V} - \nabla \cdot (\eta \nabla \boldsymbol{V}) = -\nabla P + \boldsymbol{F_\sigma} + \rho \boldsymbol{g}$ (Navier–Stokes equations)
- $\frac{\partial \alpha}{\partial t} + \boldsymbol{V} \cdot \nabla \alpha + \nabla \cdot [(\boldsymbol{V_1} - \boldsymbol{V_2})\alpha(1-\alpha)] = 0$ (Volume fraction equation)
- $\eta = \min(\eta_0, \tau_0/\dot{\gamma} + K\dot{\gamma}^{n-1})$ (Herschel–Bulkley fluid model)

$$
\begin{aligned}
\boldsymbol{V} &= \alpha \boldsymbol{V_1} + (1-\alpha)\boldsymbol{V_2} \\
\rho &= \alpha \rho_1 + (1-\alpha)\rho_2 \\
\eta &= \alpha \eta_1 + (1-\alpha)\eta_2 \\
\boldsymbol{F_\sigma} &= \sigma \kappa \nabla \alpha \\
\kappa &= -\nabla \cdot (\nabla \alpha / |\nabla \alpha|)
\end{aligned}
$$

Symbol	Description
$\boldsymbol{V}$	Velocity vector of both phases (1 & 2)
t	Time
$\boldsymbol{F_\sigma}$	Continuum surface force
σ	Surface tension
κ	Mean curvature of the free surface
α	Phase fraction ($0 \leq \alpha \leq 1$)
$\boldsymbol{g}$	Gravitational acceleration
η_0	Viscosity at a low shear rate

Assessment of Efficiency/Printability

- Extrudability and shape fidelity indicate the degree of dimensional faithfulness of the printed object vs. computer-aided design (CAD).[6]
- Analytical Model

$$D = \sqrt{\frac{4Q}{\pi V_m}}$$

Strand diameter

Volumetric flow rate

Horizontal needle moving speed

Assumptions:

I Perfect cylindrical strand

II No spreading (2D)

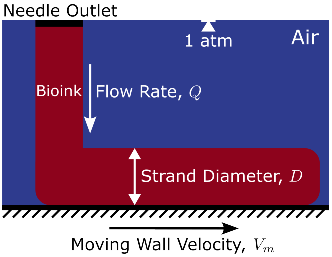

- Simulation Setup
  - $D \approx 3.57$ mm, $D_{\text{simulation}} \approx 2.90$ mm (81.1%)

[6] Schwab et al., *Chemical Reviews*, **120**(19), pp. 11028–11055, 2020

Assessment of Printability (Shape Fidelity & Shear Stress, kPa)

- Printing speed is set to 1 cm/s with a needle radius of 400 μm.
- Bioink's shape fidelity (red color) under various temperatures is compared.
- At higher temperatures (45 °C to 55 °C), bioink starts to deform easily due to low yield stress.

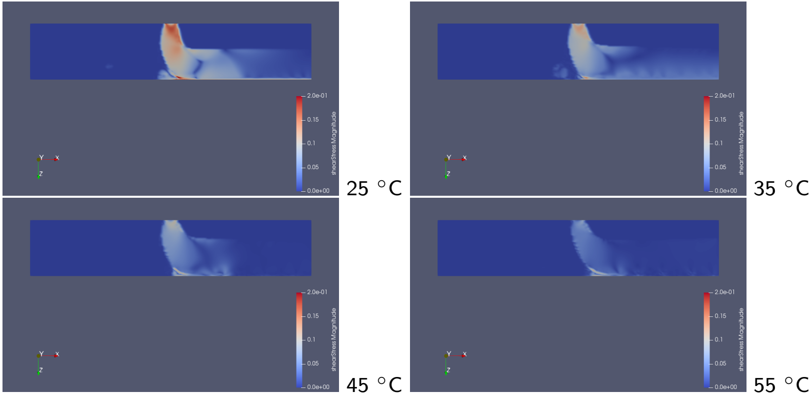

Assessment of Cell Viability (Uniform Cell Suspension)

- Existing model (R^2 of 0.859; human fibroblast; size $\sim 30\mu$m)[7]:
  - $\boxed{V_{\text{fibroblast}}(\tau_w, t_r, \eta) = 145.753 - 0.0133752 * \tau_w - 0.405308 * t_r + 0.00642919 * \eta}$
  - $t_{\text{r, simulation}} = L_n/\bar{U} \approx 130$ ms

Symbol	Description
V	Viable cells ratio (%)
τ_w	Wall shear stress (Pa)
t_r	Residence time (ms)
η	Apparent viscosity (Pa·s)

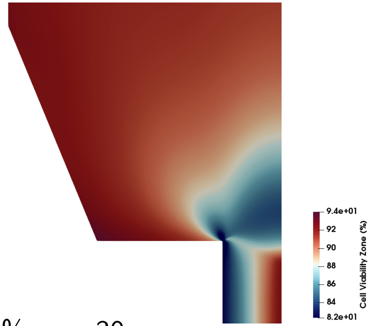

- Cell types and shear stress[8]
  - 5000 Pa $\rightarrow$ fibroblasts' viability drop below 80% over 30 ms.
  - 160 Pa $\rightarrow$ detrimental to chondrocyte's viability.

[7] Lemarié et al., *Bioprinting*, **21**(2021), e00119, 2021

[8] Webb and Doyle, *Bioprinting*, **8**(2017), pp. 8–12, 2017

Assessment of Cell Viability in Different Needle Types

- **90° Cylindrical Needle**: Exhibits a lower cell viability region primarily in the center needle inlet area, indicating a higher stress area which could harm cells.
- **45° Cylindrical Needle**: Lower cell viability is observed predominantly around the needle inlet wall, suggesting an increased cell death due to shearing stress at the interface.
- **Tapered Needle**: Shows comparatively higher cell viability across its volume, indicating its potential for higher performance in bioprinting applications.

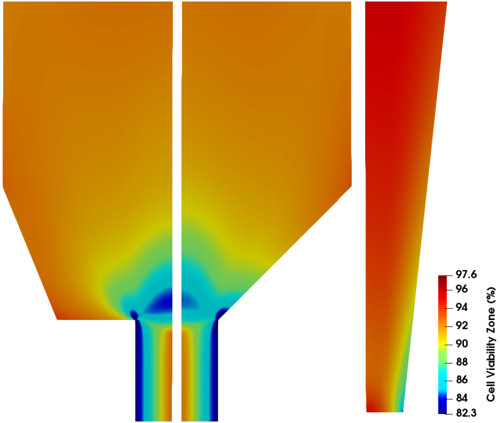

90° cylindrical, 45° cylindrical, and tapered

Conclusion

- Extensional stress (along the center needle inlet region) has the most detrimental effect on cells, despite small affected areas.
- Higher temperatures (45 °C-55 °C) reduce shear stress exerted on bioink when printing.
- Shape fidelity degrades with the temperature increase, indicating the need for a controlled printing environment.
- Among the three main factors (shear stress, residence time, and apparent viscosity) that influence cell viability, shear stress and residence time exhibit a significantly negative impact on cell viability.
- Alginate-based bioinks offer promising results due to their cost-effectiveness, biocompatibility, and easy gelation.

Next Step:

- Acquiring experimental data to train the machine learning model.
- Finalizing thesis.

References

Blaeser, Andreas et al. (2016). “Controlling Shear Stress in 3D Bioprinting is a Key Factor to Balance Printing Resolution and Stem Cell Integrity”. In: *Advanced Healthcare Materials* 5.3, pp. 326–333. ISSN: 2192-2659.

Cooke, Megan E. and Derek H. Rosenzweig (Mar. 2021). “The rheology of direct and suspended extrusion bioprinting”. In: *APL Bioengineering* 5.1, p. 011502. ISSN: 2473-2877.

Lemarié, Lucas et al. (Mar. 2021). “Rheology, simulation and data analysis toward bioprinting cell viability awareness”. en. In: *Bioprinting* 21.2021, e00119. ISSN: 2405-8866.

Piras, Carmen C. and David K. Smith (Sept. 2020). “Multicomponent polysaccharide alginate-based bioinks”. en. In: *Journal of Materials Chemistry B* 8.36, pp. 8171–8188. ISSN: 2050-7518.

Sarker, Md. and X. B. Chen (Apr. 2017). “Modeling the Flow Behavior and Flow Rate of Medium Viscosity Alginate for Scaffold Fabrication With a Three-Dimensional Bioplotter”. In: *Journal of Manufacturing Science and Engineering* 139.8, p. 081002. ISSN: 1087-1357.

Schwab, Andrea et al. (Oct. 2020). “Printability and Shape Fidelity of Bioinks in 3D Bioprinting”. In: *Chemical Reviews* 120.19, pp. 11028–11055. ISSN: 0009-2665.

Webb, Braeden and Barry J. Doyle (Dec. 2017). “Parameter optimization for 3D bioprinting of hydrogels”. en. In: *Bioprinting* 8.2017, pp. 8–12. ISSN: 2405-8866.

Zhang, Hua et al. (2020). “Direct 3D Printed Biomimetic Scaffolds Based on Hydrogel Microparticles for Cell Spheroid Growth”. en. In: *Advanced Functional Materials* 30.13, p. 1910573. ISSN: 1616-3028.

Zhang, Yu Shrike et al. (Nov. 2021). “3D extrusion bioprinting”. en. In: *Nature Reviews Methods Primers* 1.1, pp. 1–20. ISSN: 2662-8449.